Plasma–neutral interaction in thermally collapsed plasma

Jaeyoung Park *, T.K. Bennett, M.J. Goeckner, S.A. Cohen

Princeton Plasma Physics Laboratory, P.O. Box 451, Princeton, NJ 08543, USA

Abstract

A systematic experimental study of the power, length, and gas pressure dependence of plasma density and temperature profiles in thermally collapsed magnetized helium plasmas has been performed on the Princeton divertor simulator apparatus. The recombination edge and recombination radiation from highly excited levels (to $n = 12$) have been identified. The importance of radiation and neutral particles to heat transport has been demonstrated. A region of stable plasma detachment has been found and is suggested as being suitable for divertor operational space.

Keywords: Divertor simulator; Detached plasma

1. Introduction

A critical issue for the next generation tokamak is the ability to handle a very large steady-state power load in its divertor region. Currently several possible solutions, such as gas target and impurity radiation, both leading to plasma detachment, have been identified [1–7] but they have yet to be verified theoretically [8–11] or experimentally as sustainable under reactor conditions. Difficulties in understanding advanced divertor operations arise from the complexity of the plasma interacting with neutrals and impurities.

In this paper, we will present experimental results on plasma–neutral interactions in He discharges which are relevant to the gas-target concept and consequently plasma detachment. A systematic study of the particle and heat transport with respect to ambient neutral pressure, axial extension of the plasma column and input power have revealed the possibility of optimizing the divertor depth and the importance of heat transport by neutrals and radiation. Dramatically enhanced neutral emission, especially from highly excited levels, has been observed and the recombination continuum is identified.

2. Experimental setup

A plasma was produced by a lower-hybrid-wave-heated source [12] made of a coaxial cylindrical waveguide consisting of a Cu–Ni alloy center electrode and an inconel outer cylinder. Microwaves at 2.45 GHz were generated by a magnetron with the maximum output power of 2.5 kW. Input rf power coupled to the plasma was varied during the discharge between 0.1 kW to 2 kW with a control circuit in the magnetron source. Fig. 1 shows three different setups of input power variation used in the experiments. Throughout the paper, P1 denotes a single power operation (normally near the maximum power), P2 for a continuous power variation (starts high, ramps to a lower power level and then back to the high power), and P3 designates a 2 level input power variation (starts high and steps to low power). A large variation in the input power for about 80 ms at the beginning of the discharge is due to the magnetron source. All measurements are taken after about 150 ms from the start of discharges. The axial extension of the 1 cm radius plasma column was 20–40 cm long, determined by a movable end-plate which can be biased between -75 V and 75 V. This plasma column was imbedded in an uniform magnetic field of 0.35 T. Helium plasma, with density of 0.5 to 6×10^{13} cm^{-3} and the electron temperature of 3–7 eV just outside of the outer cylinder, was routinely obtained with neutral gas pressure

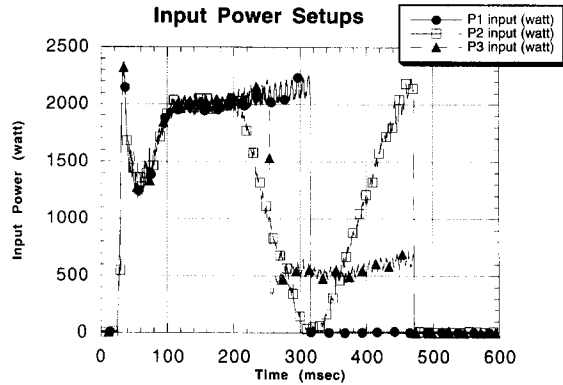* Corresponding author. E-mail: jpark@pppl.gov.

Fig. 1. Temporal behavior of input microwave power. Three different profiles are used throughout the experiments and denoted as P1, P2 and P3.

between 6.0 and 70 Pa. A more detailed description of the system setup can be found in Ref. [13].

A single Langmuir probe, which can be scanned in both the axial and radial directions with a spatial resolution of about 2 mm, was used to measure the n_e and T_e profiles. Heat flux to the target was measured by a target bolometer made of a thin copper plate (0.75 mm) with a thermocouple attached. With a MgF_2 window and a UV grade optical fiber, the emission spectrum between 250 nm and 900 nm was measured with an OMA (optical multichannel analyzer) system.

3. Experimental results

3.1. Particle flux measurement

Fig. 2 shows contour plots of target current as a function of plasma column extension and input power parameterized by the ambient neutral pressure. The target is biased to a large negative voltage compared to a floating potential, −30 V versus −5 V, to draw ion saturation current. Nine different plasma extensions, between 17 cm and 35 cm, were used. The extension of plasma column was determined as a distance from the center electrode in the source to the end-plate. For this set of experiments, the input power was varied (P2) from 2 kW to 0.2 kW and back to 2 kW during a ~ 200 ms interval, slowly enough to assure steady state at each power level. Very little hysteresis was observed in the measurements. Probe measurements at the upstream show that T_e changes less than 20% while n_e varies almost linearly with the input power. This is due to the very sensitive nature of the electron impact ionization rate to the electron temperature for He when T_e is in the range of several eV [13,14].

For He neutral pressures at 13.3 Pa, the target current increases with rf power for all plasma extensions. However, as the ambient neutral pressures increases, the increase of target current becomes much smaller for longer plasma columns. At 23.3 Pa, the target current no longer increases with the rf power for plasma columns longer than 30 cm. As the neutral pressure is increased even further, the contour plot becomes separated by two regions, one having proportionality between input power and particle flux to the target and the other with inverse proportionality.

The location of the boundary, X_B, between these two regions exhibits a special merit: plasma particle flux to the target being constant for different input power levels in the upstream region. As such, it could be utilized as the optimum condition for the divertor operation. It is not yet understood how the location of this boundary depends on the experimental conditions such as the length of the plasma column, the ambient neutral pressure, input power density, etc. However, axial T_e profile measurements by the probe relate this boundary with the onset of plasma detachment. Plasma detachment as defined in this paper is when the electron temperature in front of the target drops below 1 eV. Fig. 3 shows the axial T_e profiles at two different input power levels (P3), 2.3 kW and 0.8 kW for He discharges of 10.0 Pa and 22.1 Pa with a 30 cm plasma column length. At 22.1 Pa, the plasma column undergoes a transition from being attached at 0.8 kW to detached at 2.3 kW. However, the plasma column was attached at both power levels at 10.0 Pa with the same condition. This result is consistent with a current result from TPD1 [15], that the plasma detachment occurs with a higher electron density at the upstream.

3.2. Heat flux to the target

Absolute calibration of the heat flux to the target bolometer is done by two different methods, one from the mass and the specific heat of copper target and the other using a published value of He ion energy reflection coefficient (~ 0.3 at 10–50 eV) and a simultaneous measurement of heat flux and plasma current with varying bias voltage on the target [16,17]. The agreement between two methods was fairly good, within 20%.

Fig. 4 shows the results of heat flux and I_{sat} measurements with different plasma column extensions and ambient neutral pressures. The heat flux measurements were done with a floating target and corrected for the ion energy reflection. The measurements of I_{sat} were done with various bias voltages on the target. For these measurements, the input power coupled to the plasma was kept constant at about 2 kW (P1).

From sheath theory, the heat flux carried by the plasma can be expressed by electron temperature, ion saturation
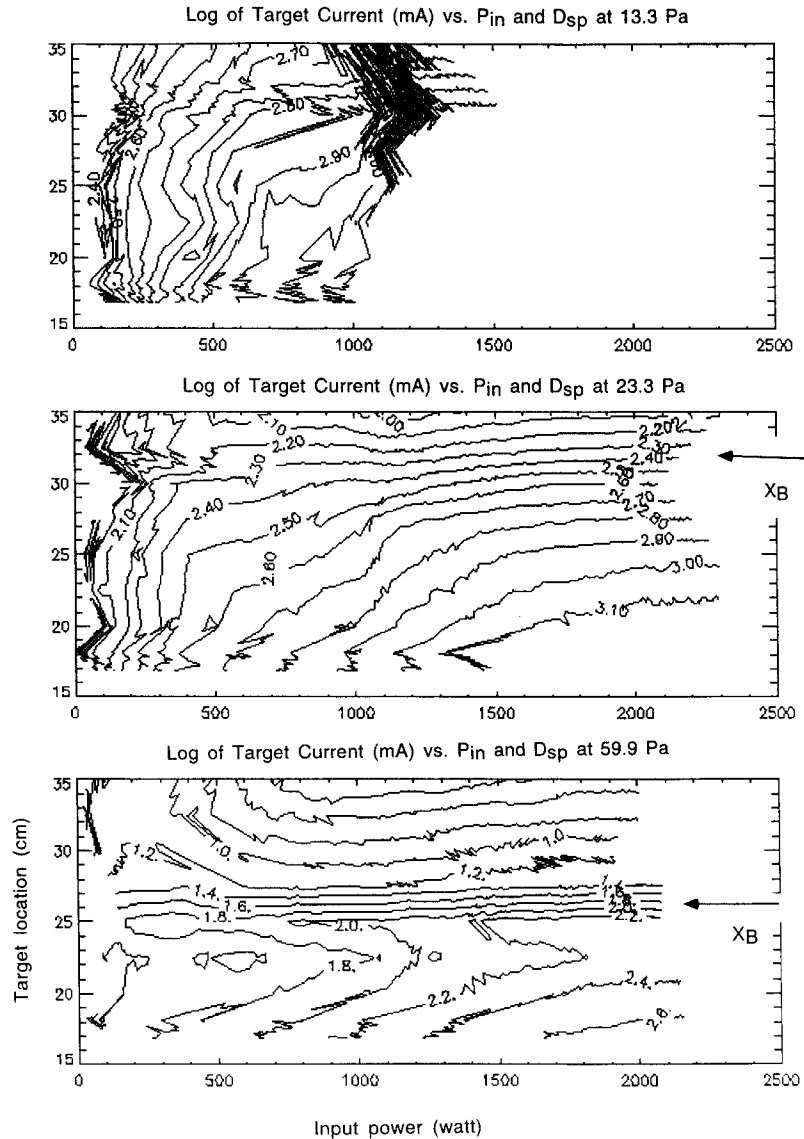
Fig. 2. 3D contour plots of the target current versus P_{in} and plasma column length at 3 different neutral pressure of 10.0 Pa, 23.3 Pa and 59.9 Pa. The target was biased to -30 V as compared to a floating potential of -5 V.

current and sheath energy transmission factor given as below [18].

$$q_{tar} = I_{sat}(\delta_t T_e + \phi_{recombination})$$ (1)

$$\delta_t = 2\tau + \frac{2}{(1-\gamma)} - 0.5 \times \ln\left[\frac{(2\pi\mu)(1+\tau)}{(1-\gamma)^2}\right],$$ (2)

where $\tau = T_i/T_e$, $\mu = m_e/m_i$, and γ is the secondary electron emission coefficient. Using $\phi_{recombination} = 24.6$ eV for He and with $T_e = 3$–0.6 eV, $T_i = 0.2$–0.5 eV and assuming $\gamma = 0.5$ for the copper target, one finds $\delta_t \sim 8$.

In Fig. 5, the ratios between q_{tar} and I_{sat} ($\delta_t T_e + \phi_{recombination}$) are plotted to compare the measured heat flux with the calculated values from T_e measurements in

front of the target. A good agreement between the two values for pressures of below 20 Pa indicates the plasma charged particles carry most of the heat flux to the target. However, as the ambient neutral pressure rises, the experimental values of heat flux become larger than those calculated from Eqs. (1) and (2). The onset of this discrepancy coincides well with the plasma detachment. This result implies that the charged particles' energy is transferred to radiation or the ambient neutrals, when detached.

3.3. Video image and optical spectrum result

Video images of the plasma column were taken and revealed a formation and a growth of a flame-like bright
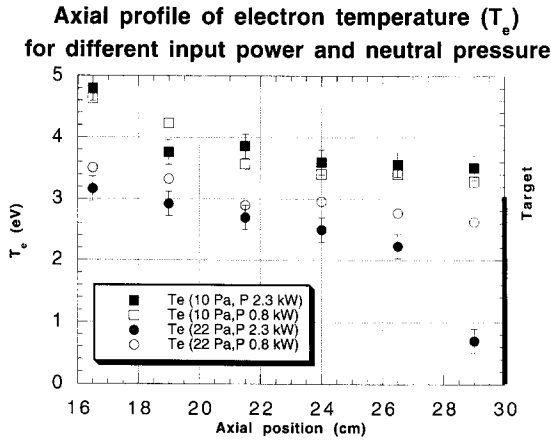
Axial profile of electron temperature (T_e)
for different input power and neutral pressure

Fig. 3. Axial profile of T_e for 2 different input power of 2.3 kW and 0.8 kW at 10.0 Pa and 22.1 Pa. Plasma column length was 30 cm and the target bias of −30 V was applied.

emission zone as the input power was increased when the experiment was setup near the boundary as discussed in Section 3.1, with the input power variation (P2). However, when the neutral pressure was lowered, leading the experimental setup away from this boundary, the increase in the input power did not produce the emission zone in the plasma column. Also, the location of this emission zone coincides closely with the region of the detached plasma in our device. Since there have been a number of reports [3,7] which relate the appearance of the emission zone with plasma detachment, the above experimental results reinforce the close relationship between X_B and the plasma detachment.

With a MgF_2 window and a UV grade fiber, the spectrum down to 250 nm has been studied by the OMA system. Emission spectrum from the radiation zone exhibits the line emission from highly excited levels, clearly n up to 12 and possibly even higher levels along with the
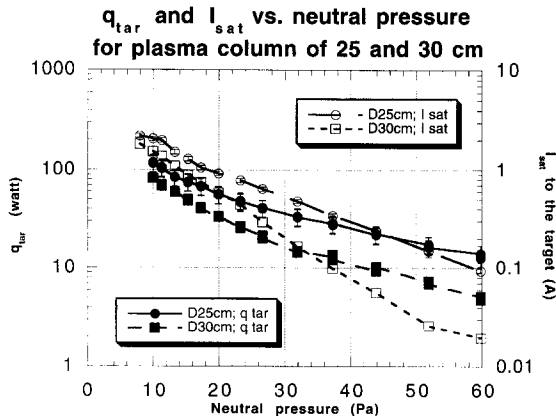
q_{tar} and I_{sat} vs. neutral pressure
for plasma column of 25 and 30 cm

Fig. 4. Heat and particle flux (I_{sat}) versus neutral pressure at different plasma column lengths of 25 cm and 30 cm.

q_{tar} / {I_{sat}(delta*T_e + 24.6)}
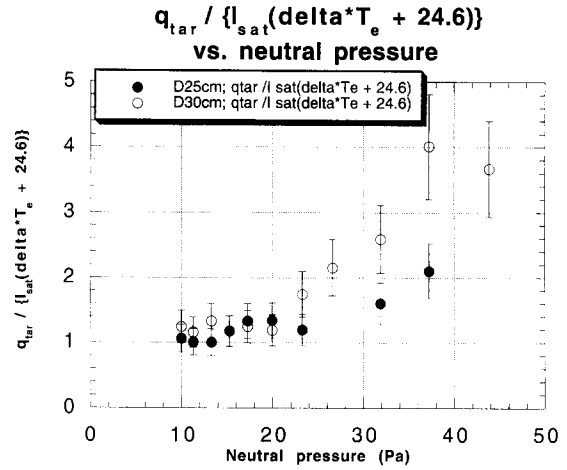**vs. neutral pressure**

Fig. 5. Ratios between q_{tar} and I_{sat} ($\delta_t T_e + \phi_{recombination}$) at two different plasma column length of 25 cm and 30 cm.

recombination continuum, as shown in Fig. 6. When compared with the results from the section of plasma column between the source and the emission zone, the increases in emission intensities are about 10–100, with the larger
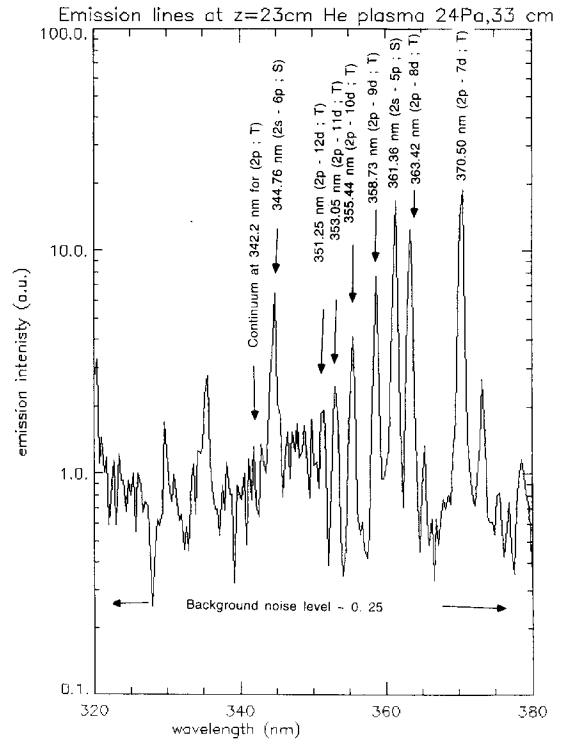

Fig. 6. Emission spectrum He plasma from $z = 23$ cm, for the discharge at 23.9 Pa, 33 cm long plasma column with P1. Emission lines from (nd–2p; T, $n = 7$, 8, 9, 10, 11 and 12) are marked and the presence of recombination continuum at 342.2 nm is suggested. Background noise is about 0.25 (au).

increases for the lines from the higher quantum states. Combined with the observation of recombination continuum, this result suggests the importance of recombination processes in the plasma detachment in our device. Recently, it has been suggested that the recombination involving hydrogen molecules may explain the plasma detachment observed in divertor tokamaks [9].

4. Summary

A systematic study of the effects of the ambient neutral pressure, plasma column extension and input power on the particle flux to the target has shown the appearance of two separate particle transport regions. The boundary between these two regions, is found to be closely related to plasma detachment and could be considered as an optimum choice of the divertor design. It is also shown that plasma detachment requires a higher input power, thus a higher electron density in the upstream, from the probe measurements and the video images. The importance of radiation and neutrals in the heat transport has been shown by the absolutely calibrated heat flux measurements. With the observation of line emission from highly excited levels and recombination continuum, the relevance of the recombination process to plasma detachment has been established.

Acknowledgements

References

[1] G.S. Chiu and S.A. Cohen, Phys. Rev. Lett. 76 (1996) 1248.
[2] W.L. Hsu et al., Phys. Rev. Lett. 49 (1982) 1001.
[3] J.A. Goetz et al., Phys. Plasmas 3 (1996) 1908.
[4] G.D. Porter et al., Phys. Plasmas 3 (1996) 1967.
[5] M.L Watkins and the JET Team, Phys. Plasmas 3 (1996) 1881.
[6] N. Ohno et al., J. Nucl. Mater. 220–22 (1995) 279.
[7] L. Schmitz et al., Phys. Plasmas 2 (1995) 3081.
[8] J. Kesner, Phys. Plasmas 2 (1995) 1982.
[9] A.Yu. Pigarov and S.I. Krasheninnikov, Phys. Lett. A., submitted.
[10] Ph. Ghendrih, Phys. Plasmas 1 (1994) 1929.
[11] M. Petravic and D.P. Stotler, J. Nucl. Mater. 220–22 (1995) 1097.
[12] R.W. Motley et al., Rev. Sci. Instrum. 50 (1979) 1586.
[13] G.S. Chiu and S.A. Cohen, Phys. Plasma., to appear.
[14] R.K. Janev et al., Elementary Processes in Hydrogen–Helium Plasmas (Springer-Verlag, 1987).
[15] N. Ezumi et al., J. Nucl. Mater. (1996), to appear.
[16] G. Fiksel, Ph.D. thesis, University of Wisconsin–Madison (1991).
[17] Ito et al., Data on the Backscattering Coefficients of Light Ions from Solids (A Revision), Report of Institute of Plasma Physics, Nagoya University, IPPJ-AM-41 (1985).
[18] P.C. Stangeby, Phys. Fluids 27 (1984) 682.